

# Neutron-Scattering Analysis of the Linear-Displacement Correlations in $\text{KTaO}_3$ <sup>†</sup>

R. Comès\* and G. Shirane

*Brookhaven National Laboratory, Upton, New York 11973*

(Received 1 September 1971)

In view of recent x-ray experiments which detected a surprisingly strong diffuse scattering in the  $\{100\}$  reciprocal sheets of  $\text{KTaO}_3$ , a new neutron-scattering investigation was performed to determine the origin of this scattering. It was found that a strong anisotropy in the dispersion of the low-lying phonon branches, which was unexpected from the earlier data, can account for the x-ray results. Both the transverse-acoustic and lower-optic phonons polarized along  $[010]$  have particularly low frequencies in the reciprocal  $\{100\}$  sheets. This anisotropy of the dispersion relation can be understood as arising from dipolar-type forces along the  $\langle 100 \rangle$  directions, and optic-acoustic mode interaction restricted to the same directions.

## I. INTRODUCTION

$\text{KTaO}_3$  along with  $\text{SrTiO}_3$  was one of the first examples for which neutron scattering provided unambiguous experimental evidence that ferroelectric phase transformations are associated with an instability of a long-wave optical phonon<sup>1</sup> as predicted by Cochran.<sup>2</sup> Earlier experiments on  $\text{KTaO}_3$ ,<sup>1,3</sup> which were restricted to a few high-symmetry directions, suggested that  $\text{KTaO}_3$  had quite normal dynamical properties as far as the anisotropy was concerned. This differed from other ferroelectric perovskites as  $\text{BaTiO}_3$  or  $\text{KNbO}_3$ , where strong correlations of the atomic displacements along the  $\langle 100 \rangle$  directions<sup>4,5</sup> give rise to a particularly anisotropic dispersion spectrum.<sup>6-8</sup> Furthermore,  $\text{KTaO}_3$  has undamped soft optic modes which give rise to well-defined energy peaks, in contrast with the damped or even overdamped behavior of the lower-optic modes in the true ferroelectric perovskites as  $\text{BaTiO}_3$  or  $\text{KNbO}_3$ .<sup>7,8</sup>

Recent x-ray-scattering results<sup>9</sup> have nevertheless shown that, as is the case with  $\text{BaTiO}_3$  and  $\text{KNbO}_3$  in their cubic phases,  $\text{KTaO}_3$  shows a strong diffuse scattering restricted to the three sets of  $\{100\}$  reciprocal sheets. This implies that correlation phenomena along the  $\langle 100 \rangle$  directions also exist in that crystal. The sheets in  $\text{KTaO}_3$  are slightly broader than in  $\text{KNbO}_3$ , thus showing a somewhat shorter correlation range. These sheets are not limited to small values of the wave vector  $\vec{q}$  near the zone center, but extend to the entire Brillouin zone, with a relatively constant intensity. Their intensity was found to be approximately proportional to the Kelvin temperature.

This result was totally unexpected, and in view of the important role such correlations are believed to play in the ferroelectric properties and in the mechanism of the ferroelectric phase transformation of the perovskite crystals,<sup>10-12</sup> a new neutron-scattering analysis of  $\text{KTaO}_3$  was felt necessary to

determine the nature of this particular x-ray scattering.

In this paper, we report the results with a special emphasis on the eventuality of an anisotropic quasielastic scattering and the possibility of an important anisotropy of the lower-frequency dispersion branches.

## II. EXPERIMENTAL

The measurements were performed at the Brookhaven high flux beam reactor, utilizing a triple-axis spectrometer, with pyrolytic graphite crystals used as monochromator and analyzer.<sup>13</sup> Constant- $Q$  and constant- $E$  techniques were employed with incoming energies of 5, 13.8, and 38 meV.

The  $\text{KTaO}_3$  single crystal purchased from Sanders Associates<sup>14</sup> was grown by the top-seeded solution method and had a volume of approximately  $1 \text{ cm}^3$ . Rocking curves measured in the  $(hk0)$  reciprocal-lattice plane gave an effective mosaic spread of  $0.16^\circ$  (full width at half-maximum).

At first we searched for the origin of the x-ray scattering sheets as due to additional quasielastic scattering around  $\Delta E = 0$ . As shown in Fig. 1, we did find a strongly  $\vec{q}$ -dependent quasielastic scattering. Two experimental facts nevertheless clearly indicate that even though this additional cross section might be related to the x-ray results, it cannot explain the x-ray diffuse sheets: (a) This quasielastic scattering is practically independent of temperature. (b) It is restricted to the vicinity of the Brillouin-zone center.

Our next step was to investigate in detail the anisotropy of the lowest acoustic- and optic-dispersion branches as a function of the directions of the wave vector  $\vec{q}$  and of the eigenvector  $\vec{e}$ . As we shall see in Sec. III, this approach was successful in explaining the x-ray diffuse sheets as well as shedding new light on the basic characteristics of perovskite-type ferroelectrics.

As for the quasielastic cross section at small

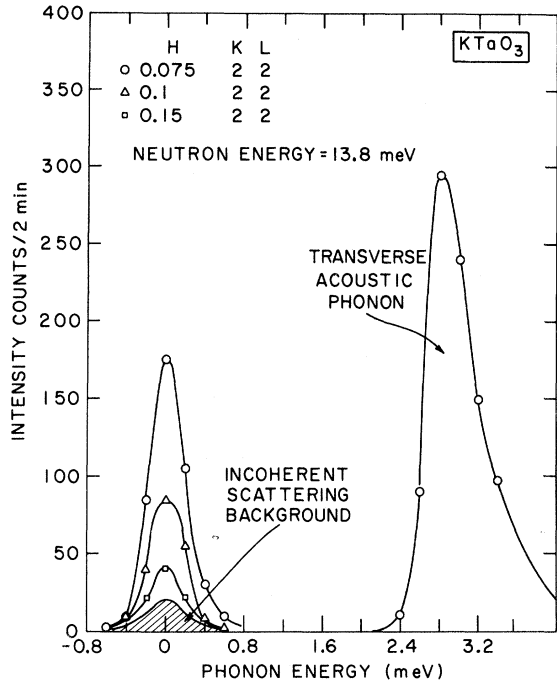


FIG. 1. Compared scattering profiles of the transverse-acoustic phonon and of the particular quasielastic scattering found in the vicinity of the  $\{100\}$  sheets and near the Bragg peaks.

wave vectors, we do not have at present any plausible explanation. A few more pertinent comments will be made in Sec. V about this point.

### III. ANISOTROPY OF DISPERSION BRANCHES

Figure 2 shows the measured dispersion curves along three directions:  $[110]$  ( $T_2$  mode polarized  $[\bar{1}, 1, 0]$ ),  $[100]$ , and along a direction at  $15^\circ$  from  $[100]$  in the  $(hk0)$  zone. The acoustic and optic branches along  $[100]$  are found to be in good agreement with previous results.<sup>3</sup> The striking feature which arises from the comparison of the dispersion along different directions is that both the transverse-optic and the transverse-acoustic branches are found to have a pronounced frequency dip along the  $[100]$  direction. This frequency dip is better visualized if we consider several plane sections perpendicular to  $[100]$  of the dispersion spectrum as shown in Fig. 3. The difference between the shape of the sections of the transverse-acoustic and optic-dispersion curves and that of the longitudinal-acoustic branch which has a normal  $q$  dependence should in particular be noted.

The above-mentioned data restrict the lowest values of the frequencies of the transverse-acoustic and optic-dispersion branches to the  $\langle 100 \rangle$  reciprocal directions, while the x-ray scattering was found in whole  $\{100\}$  reciprocal sheets, namely, any point on such a sheet corresponds to a wave vector  $\vec{q}$  perpendicular to a  $\langle 100 \rangle$  direction and to a polarization vector  $\vec{e}$  parallel to the same  $\langle 100 \rangle$  direction. Additional data along the  $[101]$  direction ( $T_1$  mode polarized  $[010]$ ) and along the  $[111]$  direction are thus needed for a more complete comparison of the neutron-scattering data with the x-ray results.

As shown from the dispersion curves of Fig. 4,

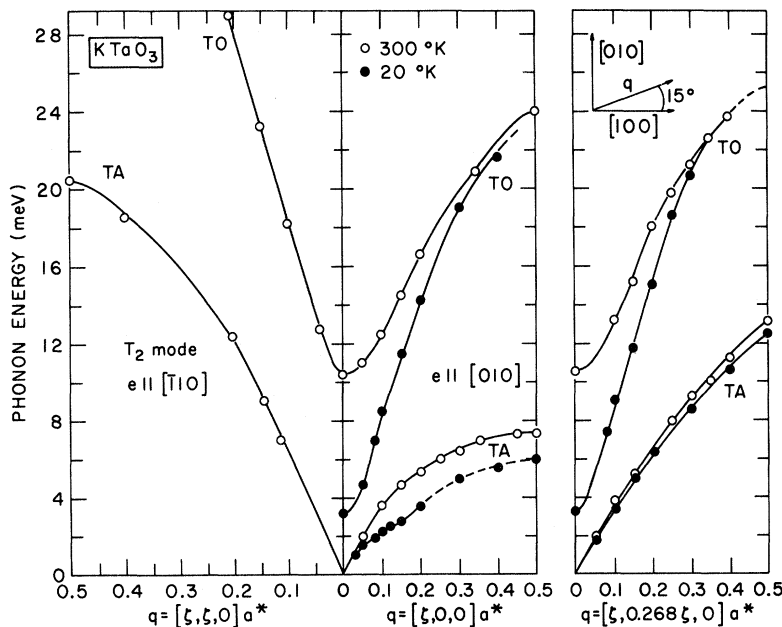


FIG. 2. Transverse-acoustic and optic-dispersion curves along  $[110]$  ( $T_2$  mode polarized  $[\bar{1}, 1, 0]$ ),  $[100]$ , and along a straight line at  $15^\circ$  from  $[100]$ . In the two latter cases the  $20^\circ\text{K}$  curves are also shown.

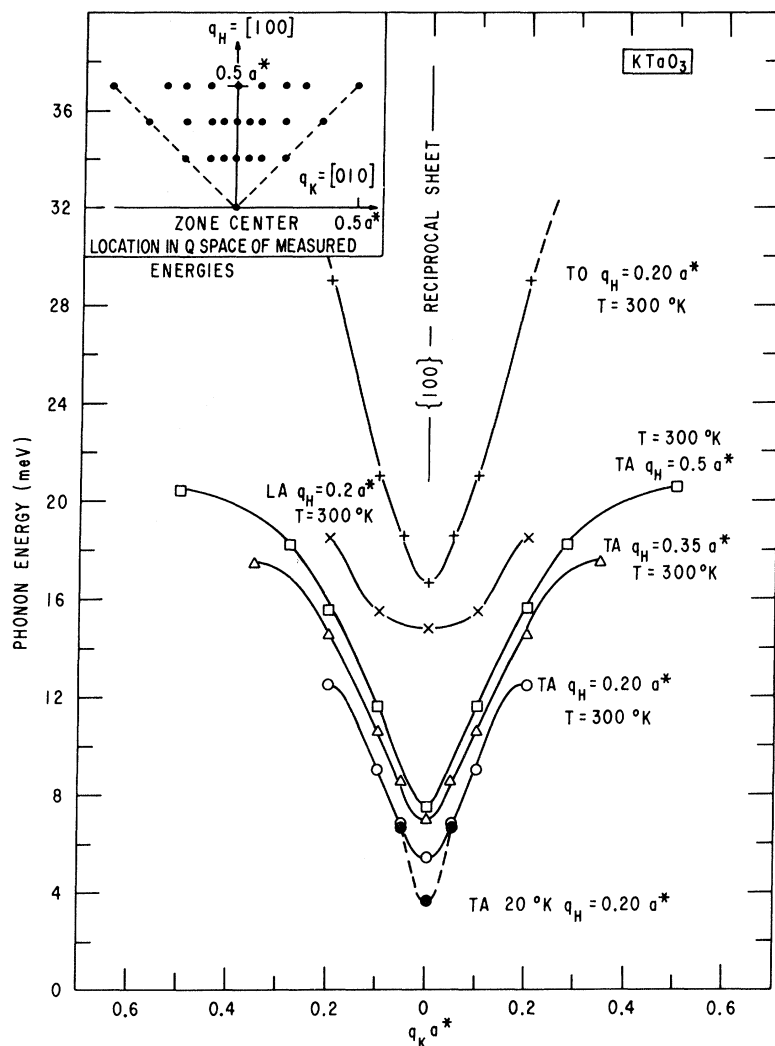


FIG. 3 Plane section perpendicular to  $[100]$  of the dispersion spectrum. Note the smooth variation of the longitudinal-acoustic mode compared to the pronounced dip of the transverse-acoustic and lower-optic modes.

the lower values of the frequencies of the transverse-optic and transverse-acoustic branches extend to the  $[101]$  direction for phonons polarized along  $[010]$ . The anisotropy is even found to be slightly more pronounced around  $[101]$  than around the  $[100]$  direction. This thus establishes that both the transverse-acoustic and transverse-optic modes polarized along  $\langle 010 \rangle$  have exceptionally low frequencies.

In the light of such a pronounced anisotropy it appeared useful to get some additional low-temperature data. When the temperature is lowered to  $20^\circ\text{K}$  the anisotropy of the acoustic branch is found to increase. The whole branch, in agreement with previous data,<sup>3</sup> shows a pronounced frequency decrease. Figure 2 shows that this anomalous effect is narrowly restricted to the  $[100]$  direction, since only a much smaller change is detected along the direction at  $15^\circ$  from  $[100]$ . The anomalous temperature dependence of both the acoustic and transverse-optic modes of  $\text{KTaO}_3$  was already observed

by Axe, Harada, and Shirane<sup>3</sup> along the  $[100]$  direction, and successfully explained in the long-wavelength limit by an optic-acoustic mode interaction. Figure 5 illustrates the characteristic dispersion curves, at  $20^\circ\text{K}$ , and for small wave vectors, along the  $[100]$  direction and along the direction at  $15^\circ$  from  $[100]$ . The pronounced dip on the  $[100]$  transverse-acoustic branch at  $q = 0.15a^*$  ( $a^* =$  reciprocal lattice parameter) was previously explained<sup>3</sup> by the strong optic-acoustic mode interaction. Note that this dip is entirely missing for the transverse-acoustic branch along the direction at  $15^\circ$  from  $[100]$ . This clearly demonstrates that the mode interaction is the main cause of the steep anisotropy of the acoustic dispersion.

In this respect it is interesting to examine the anisotropy of the initial slope of the dispersion curves; since the mode interaction is roughly proportional to  $q^2$ , it should disappear as  $q$  approaches zero. The transverse velocities at room tempera-

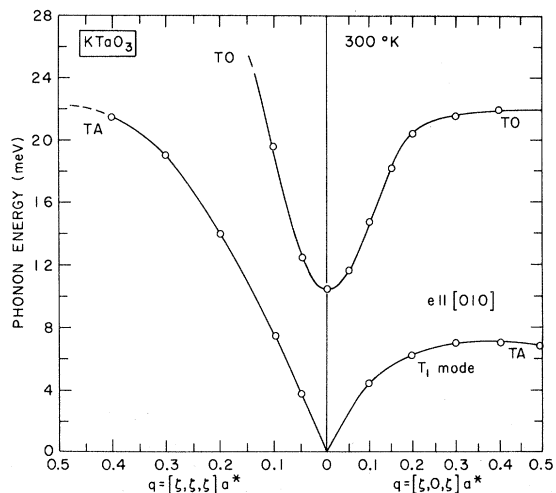


FIG. 4 Transverse-acoustic and optic-dispersion curves along [101] ( $T_1$  mode polarized [010]) and along [111]. Note the extension of the horizontal part of the branches near the zone boundary along [101], that is, for the direction where the frequency is lowest.

ture are  $3.909(\pm 0.01)10^5$  cm/sec along [100],<sup>15</sup> and  $4.34(\pm 0.2)10^5$  cm/sec along [110], which indeed shows that the anisotropy of the transverse-acoustic branch is very small at  $q=0$ .

It should, furthermore, be noted that with the additional available data about the acoustic dispersion, the three first-order elastic constants for  $\text{KTaO}_3$  can now be deduced from the neutron-scattering experiments alone<sup>1,3</sup> (in  $10^{12}$  dyn/cm<sup>2</sup>):  $c_{44} = 1.15(\pm 0.06)$ ,  $c_{11} = 4.04(\pm 0.1)$ ,  $c_{12} = 1.40(\pm 0.07)$ . These are to be compared with the values obtained by Barrett<sup>15</sup> from ultrasonic attenuation measurements (in  $10^{12}$  dyn/cm<sup>2</sup>):  $c_{44} = 1.071$ ,  $c_{11} = 3.936$ . Using this latter more precise value of  $c_{11}$  and the neutron data for the acoustic  $T_2$  dispersion branch one gets for the third elastic constant  $c_{12} = 1.30 \times 10^{12}$  dyn/cm<sup>2</sup>.

#### IV. ANISOTROPY OF PHONON CROSS SECTION

The anisotropy of the measured inelastic cross sections is of particular importance if one wishes to compare the neutron- with the x-ray scattering data, as this latter technique is only sensible to the intensity anisotropy. The integrated intensity of a constant- $Q$  scan through a dispersion branch  $j$  at constant temperature is approximately proportional to  $F_j(Q)/\hbar\omega_j^2$ , where  $F_j$  is the inelastic structure factor and  $\omega_j$  the phonon frequency.

If we could assume that the structure factor itself does not vary significantly in the immediate vicinity of the {100} sheets, the anisotropy of the cross sections to be expected for the transverse-acoustic and transverse-optic phonons along the [100] directions could be calculated from the fre-

quency anisotropy alone. Such a simple picture is nevertheless altered by the optic-acoustic interaction. This can be seen in Fig. 6, where the neutron cross sections, calculated with the more appropriate formula and assuming constant structure factors in the vicinity of the {100} sheets, are compared to the measured cross sections in different Brillouin zones and along a line which goes across a {100} sheet. To allow such a comparison the calculated and measured cross sections were normalized to 1 at a distance of  $0.1a^*$  from the (100) sheet (where the interaction is already known to be negligible). Compared to what is expected from the frequency anisotropy, the measured cross-section anisotropy is either enhanced or reduced according to the mode which is considered (optic or acoustic) and to the Brillouin zone where the measure is performed. The enhanced or reduced cross sections along the [100] direction are in agreement with the cross sections calculated by Axe *et al.*<sup>3</sup> from the temperature-dependent mode interaction, and the curves of Fig. 6 provide another way to show that the mode interaction is restricted to [100] directions.

This shows that even in the extreme case of the 400 Brillouin zone which corresponds to the most

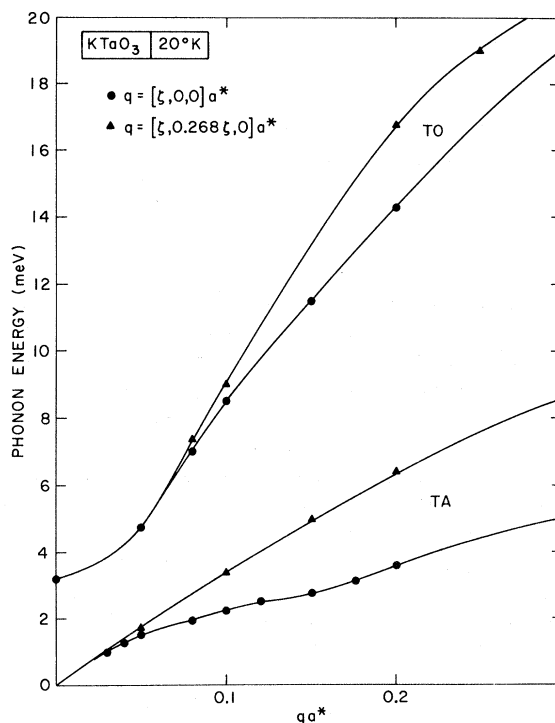


FIG. 5. Transverse-acoustic and optic-dispersion curves at 20°K and for small wave vectors, along the [100] direction and a line at 15° from it. Note that the anomalous  $q$  dependence is restricted to the [100] direction.

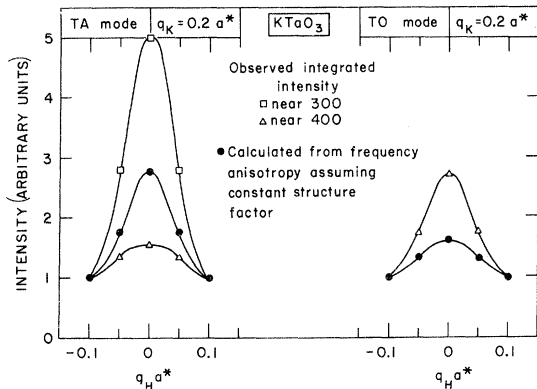


FIG 6. Comparison along a line perpendicular and across the  $\{100\}$  sheet, of the variation of the measured integrated cross sections of the acoustic and optic modes in different Brillouin zones, with the variation expected from the frequency dip assuming constant structure factors. All curves are normalized to 1 at a distance  $q = 0.1 a^*$  from the sheet.

pronounced reduction of the anisotropy of the neutron cross section for the acoustic branch, there is a well-defined intensity peak in the  $(100)$  sheet. Replacing the neutron-scattering length by the x-ray scattering factors in the cross sections calculated by Axe *et al.*<sup>3</sup> from the optic-acoustic mode interaction, it is found that such an extreme reduction of the anisotropy of the acoustic cross section never occurs in the x-ray case. There is thus no doubt that the anisotropy of the transverse-acoustic branch, which because of its lower frequency has higher cross sections than the transverse-optic branch, can at least qualitatively account for x-ray diffuse scattering found in the  $\{100\}$  sheets.

So far we have only considered the variation of the neutron cross sections along a line which goes across a  $\{100\}$  sheet. Considering the measured cross sections in such a sheet and along a  $\langle 100 \rangle$  direction, in the 300 zone, one finds that the integrated intensity of the transverse-acoustic phonon peak at the zone boundary ( $q = 0.5 a^*$ ) is still 75% of the intensity measured at  $q = 0.2 a^*$ , showing a very small  $q$  dependence which is in agreement with one of the puzzling aspects of the x-ray diffuse scattering.

## V. DISCUSSION

The present results show that the linear correlation of the atomic displacement along the  $\langle 100 \rangle$  directions, which give rise to the diffuse sheets observed with x rays in KTaO<sub>3</sub>, are dynamic.

The most obvious anisotropic forces which can be invoked in an attempt to understand such anisotropic properties are dipolar interactions. When a Ta atom is displaced, its dipole field polarizes the surrounding atoms and the next Ta ion will be

displaced due to the direct dipole field of the first Ta atom and the indirect polarization field of the surrounding atoms. This gives rise to correlated displacements which are most likely along the  $\langle 100 \rangle$  directions where the Ta-O-Ta succession of positive and negative ions and the shortest Ta-Ta distance favor such a mechanism, which was suggested long ago by Slater.<sup>16</sup> Because of the rapid decrease of the electric field away from the dipolar chain which thus arises, one can understand that the next parallel chain is not much influenced and can experience another parallel but possibly opposite polarization. Such a tendency of correlated movements of the atoms along each single  $\langle 100 \rangle$  array of atoms can then account for a much lower frequency of the lowest transverse-optic mode in the  $\{100\}$  sheets, as found experimentally. This is essentially what Hüller<sup>17,18</sup> has shown in a simple theoretical model applied to the soft-phonon dispersion in BaTiO<sub>3</sub>. It is in particular striking that Hüller's calculations predict the strongest anisotropy of the optic mode to occur in the  $\langle 101 \rangle$  directions, which is precisely what is found experimentally, as can be seen by comparing Figs. 2 and 4; the effect is nevertheless smaller than predicted.

At present there is no theoretical model to explain the anisotropy of the transverse-acoustic branch which undoubtedly gives the most important contribution to the x-ray scattering. But we have shown that this anisotropy is greatly enhanced by the optic-acoustic mode interaction.

If we now compare the available neutron- and x-ray-scattering results for different perovskites, KTaO<sub>3</sub> is the first example where a dispersion spectrum which is well defined in energy (undamped modes) can account for very anisotropic correlations of the atomic displacements. In all other cases where both techniques have already been used, linear correlations<sup>5</sup> or planar correlations as in KMnF<sub>13</sub><sup>19</sup> were accompanied by heavily damped modes<sup>7,8,20</sup> illustrating even more complex dynamical properties. Such a simple behavior of KTaO<sub>3</sub> may be related to the fact that this crystal does not undergo a phase transition, and that in contrast to crystals like BaTiO<sub>3</sub> or KNbO<sub>3</sub>, where the consideration of the ionic radii shows that the space available for the Ti or Nb ions is slightly too large, the Ta ion in KTaO<sub>3</sub> is slightly too big and is thus more tightly bound.

Another surprising result of the actual data is the extreme flatness of the  $\langle 100 \rangle$  polarized transverse dispersion branches in the  $\{100\}$  sheets and near the zone boundary. Such flat dispersion curves provide extremely high density of states and might explain the occurrence of particularly intense second-order Raman scattering.<sup>21</sup>

We are now left with one unsolved problem about the neutron scattering from KTaO<sub>3</sub>, namely, the

quasielastic scattering shown in Fig. 1. The origin of this scattering is not at all understood at present. Moreover, we even failed to characterize this scattering precisely. Its location in energy is well centered at  $E=0$ ; however, its location in reciprocal space is not exactly along the  $\{100\}$  sheets and varies from one Brillouin zone to another in a way which cannot be explained from the present knowledge of the triple-axis spectrometer resolution function.<sup>22</sup> Preliminary study of other perov-

skites  $\text{KMnF}_3$  and  $\text{SrTiO}_3$  near the zone center indicates that this scattering is rather common in perovskite crystals. This poses a rather intriguing question for further investigation of this type of crystals.

#### ACKNOWLEDGMENT

We would like to express our thanks to Dr. J. D. Axe for many illuminating discussions.

<sup>†</sup>Work supported by the U. S. Atomic Energy Commission and the National Science Foundation.

\*Guest scientist on leave from Service de Physique des Solides associé au CNRS, Faculté des Sciences, 91-Orsay, France (now returned).

<sup>1</sup>G. Shirane, R. Nathans, and V. J. Minkiewicz, *Phys. Rev.* **157**, 396 (1967).

<sup>2</sup>W. Cochran, *Advan. Phys.* **9**, 387 (1960).

<sup>3</sup>J. D. Axe, J. Harada, and G. Shirane, *Phys. Rev. B* **1**, 1227 (1970).

<sup>4</sup>G. Honjo, S. Kadera, and N. Kitamura, *J. Phys. Soc. Japan* **19**, 351 (1964).

<sup>5</sup>R. Comès, M. Lambert, and A. Guinier, *Acta Cryst.* **A26**, 244 (1970).

<sup>6</sup>Y. Yamada and G. Shirane, *Phys. Rev.* **177**, 848 (1969).

<sup>7</sup>J. Harada, J. D. Axe, and G. Shirane, *Phys. Rev. B* **4**, 155 (1971).

<sup>8</sup>A. C. Nunes, J. D. Axe, and G. Shirane, *Ferroelectrics* (to be published).

<sup>9</sup>R. Comès, F. Dénoyer, and M. Lambert, *J. Phys. Suppl.* (to be published).

<sup>10</sup>S. H. Wemple, *Phys. Rev. B* **2**, 2679 (1970).

<sup>11</sup>M. E. Lines, *Phys. Rev. B* **2**, 690 (1970).

<sup>12</sup>M. Lambert and R. Comès, *Solid State Commun.* **7**, 305 (1969).

<sup>13</sup>T. Riste and K. Otnes, *Nucl. Instr. Methods* **75**, 197 (1969).

<sup>14</sup>Sanders Associates, 95 Canal Street, Nashua, N. H. 03060.

<sup>15</sup>H. H. Barrett, *Phys. Letters* **26A**, 217 (1968).

<sup>16</sup>J. C. Slater, *Phys. Rev.* **78**, 748 (1950).

<sup>17</sup>A. Hüller, *Z. Physik* **220**, 145 (1969).

<sup>18</sup>A. Hüller, *Solid State Commun.* **7**, 589 (1969).

<sup>19</sup>R. Comès, F. Dénoyer, L. Deschamps, and M. Lambert, *Phys. Letters* **34A**, 65 (1971).

<sup>20</sup>K. Gesi, J. D. Axe, G. Shirane, and A. Linz, *Phys. Rev. B* (to be published).

<sup>21</sup>W. G. Nielsen and J. G. Skinner, *Phys. Rev.* **47**, 1413 (1967).

<sup>22</sup>M. J. Cooper and R. Nathans, *Acta Cryst.* **23**, 357 (1967).

## Piezo Soft X-Ray Effect in Nickel

R. H. Willens and D. Brasen

*Bell Laboratories, Murray Hill, New Jersey 07974*

(Received 4 May 1971)

The modulation of the  $L_{III}$  x-ray emission band of nickel due to an alternating mechanical strain is reported. Structure previously not seen in the normal x-ray emission is now resolved, which enables determination of the location of the Fermi energy and other critical points or Van Hove singularities. The bottom of the  $d$  band is placed at  $5.5 \pm 1.0$  eV from the Fermi energy. Structure which can be correlated with the spin-exchange energy places its value at  $0.68 \pm 0.1$  eV. The high-energy tails of the  $L_{II}$  and  $L_{III}$  emission bands contain a satellite which is resolved in the modulation spectrum. The origin of this satellite is attributed to spin-polarization exchange with the  $2p$  core states. The experimentally determined value of this exchange is  $5.5 \pm 0.5$  eV.

### I. INTRODUCTION

Recently, the modulation of the  $L_{III}$  emission spectrum of copper due to an alternating elastic strain was reported.<sup>1</sup> The gross shape of the modulation curve, in the first approximation, had the appearance of the derivative of the emission band. However, superimposed on this curve was additional

structure which was associated with positions in the  $3d-4s$  band of copper which were extra sensitive to strain as regards altering the x-ray emission. These positions were identified with the Fermi energy and Van Hove singularities or critical points.

The  $L_{III}$  emission spectrum of nickel (Fig. 1), which corresponds to transitions from the  $3d-4s$  band to the  $2p_{3/2}$  core level, is essentially struc-